Stopped-Flow Fluorescence Study of Precatalytic Primer Strand Base-Unstacking Transitions in the Exonuclease Cleft of Bacteriophage T4 DNA Polymerase†

Michael R. Otto,‡,§ Linda B. Bloom,||,⊥ Myron F. Goodman,|| and Joseph M. Beechem*,‡

Department of Molecular Physiology and Biophysics, Vanderbilt University, Nashville, Tennessee 37232, and Department of Biological Sciences, HEDCO Molecular Biology Laboratory, University of Southern California, Los Angeles, California 90089-1340

Received January 9, 1998; Revised Manuscript Received May 15, 1998

ABSTRACT: DNA polymerases are complex enzymes which bind primer−template DNA and subsequently either extend or excise the terminal nucleotide on the primer strand. In this study, a stopped-flow fluorescence anisotropy binding assay is combined with real-time measurements of a fluorescent adenine analogue (2-aminopurine) located at the 3′-primer terminus. Using this combined approach, the exact time course associated with protein binding, primer terminus unstacking, and base excision by the 3′ → 5′ exonuclease of bacteriophage T4 (T4 pol) was examined. T4 pol binding and dissociation kinetics were found to obey simple kinetics, with identical on rates ($k_{on} = 4.6 \times 10^8$ M^{-1} s^{-1}) and off rates ($k_{off} = 9.3$ s^{-1}) for both single-stranded primers and double-stranded primer−templates (at 100 μM Mg^{2+}). Although the time course for T4 pol−DNA association and dissociation obeyed simple kinetics, at suboptimal Mg^{2+} concentrations (e.g., 100 μM), non-first-order sigmoidal kinetics were observed for the base-unstacking reaction of the primer terminus in double-stranded primer−templates. The observed sigmoidal kinetics for base unstacking demonstrate that T4 pol is a hysteretic enzyme [Frieden, C. (1970) *J. Biol. Chem. 245*, 5788−5799] and must exist in two DNA bound conformations which differ greatly in base-unstacking properties. A Mg^{2+}-dependent time lag of 10 ms is observed between primer−template binding and the beginning of the unstacking transition, which is 50% complete at 22 ± 1 ms after addition of 100 μM Mg^{2+}. Following the hysteretic lag, a simple first-order primer terminus unstacking rate of 130 s^{-1} is resolved, which is protein and Mg^{2+} concentration-independent. For the processing of single-stranded primers, all kinetic complexity is lost, and T4 pol binding and primer end base-unstacking kinetics can be superimposed. These data reveal that the kinetic processing of double-stranded primer−template DNA by T4 pol is much more complex than that of single-stranded primers, and suggest that the intrinsic "switching rate" between the polymerase and exonuclease sites may be much faster than previously proposed.

Time-resolved and steady-state fluorescence equilibrium studies of 2-aminopurine (2AP)[1] containing DNA revealed spectroscopic and biochemical evidence for the existence of multiple populations of 3′-primer termini when it is bound to T4 DNA polymerase (*1*). The multiple populations were interpreted in terms of an equilibrium distribution of primer termini in both the polymerase and exonuclease active sites of this enzyme. While careful equilibrium studies can provide important information concerning the existence of multiple enzyme−substrate conformational states, these studies cannot provide direct information concerning the mechanism or sequence by which these states are connected. To obtain this information, pre-steady-state stopped-flow fluorescence experiments were performed.

Many classes of proteins are required to bind DNA, translocate to a specific site, and induce a structural transition or catalyze a reaction in DNA at that site. Following each of these transitions with high sensitivity and in real time is difficult. To be able to investigate real-time binding as well as real-time base unstacking in T4 pol, a "two-color" fluorescence assay system involving rhodamine-X and 2AP was developed [see Figure 1 of the preceding paper (*1*)]. Using this approach, it is possible to simultaneously monitor the binding, primer terminus base unstacking, and exonuclease kinetics of a DNA polymerase reaction in real time.

The kinetics of binding of the 104 kDa T4 pol onto a 17mer−30mer primer−template (p/t) is quantitated using stopped-flow fluorescence anisotropy changes of extrinsically labeled DNA (*2*−*4*). The coupling between DNA binding, internal base unstacking, and exonucleolytic catalysis is directly examined by correlating changes in fluorescence anisotropy with changes in the fluorescence properties of 2AP as it is processed and cleaved from the 3′-terminus of site-specifically labeled single-stranded (ss) and double-

† This work was supported by NIH Grants GM45990, RR5823 (J.M.B.), and GM21422 (M.F.G.).

* Corresponding author.
‡ Vanderbilt University.
§ Present address: Axiom Biotechnologies, San Diego, CA 92121.
|| University of Southern California.
⊥ Present address: Department of Chemistry, Arizona State University, Tempe, AZ 85287.

[1] Abbreviations: 2AP, 2-aminopurine; DTT, dithiothreitol; T4 pol, wild-type T4 DNA polymerase; p/t, 17mer−30mer primer−template DNA; ss, single-stranded; ds, double-stranded.

S0006-2960(98)00075-0 CCC: $15.00
Published on Web 06/25/1998

stranded (ds) DNA. The fluorescence intensity of 2AP within DNA is significantly different among ss DNA, ds DNA, T4 pol-bound DNA, and cleaved monophosphate (*1*, *5*−*7*), allowing a variety of real-time fluorescence signal changes to be monitored. The advantage of using 2AP fluorescence to monitor T4 polymerase exonucleolytic transitions is that the fluorescence signal originates from the nucleotide base which is being processed and cleaved, allowing a direct visualization of a variety of intramolecular steps which may be essentially invisible in radioligand studies. These pre-steady-state kinetic studies also provide an important additional level of support for the multisite interpretation of the equilibrium data from the preceding paper (*1*).

Despite being the replication polymerase from a bacteriophage, this DNA polymerase is homologous in sequence to (*8*, *9*) and shares similarities in the structure and function of its replication accessory proteins (*10*) with a large family of DNA polymerases which includes human replicative DNA polymerases. Hence, mechanistic information obtained for this enzyme may provide a conceptual framework in which to interpret the polymerase and exonucleolytic properties of a wide variety of DNA polymerase systems.

EXPERIMENTAL PROCEDURES

Materials

Preparation of WT and Mutant Polymerases. Wild-type T4 DNA polymerase and the exonuclease-deficient D112A/E114A DNA pol were prepared and purified as described previously (*11*). T4 polymerase concentrations were determined by the absorbance at 280 nm [1.492×10^5 M^{-1} cm^{-1} (*12*)]. Each enzyme preparation was titrated with 2AP-containing DNA (in the presence of EDTA) to determine the concentration of T4 pol necessary to completely saturate DNA primer−templates (*7*).

Preparation of Oligonucleotides. Oligonucleotides were prepared using standard β-cyanoethyl phosphoramidite reagents from Applied Biosystems. 2AP was incorporated at the 3′-end of primers using an 2AP-derivatized CPG (*13*). The sequence of the primer strand is 5′-TCCCAGTCACGACGTC-2AP and that for the template strand 3′-AGGGTCAGTGCTGCAGTAGTACGAGCTAC. The 17mer primer for extrinsic fluorescence labeling (same sequence that was described for the 2AP-containing primer) was synthesized with a nonhydrolyzable 3′-phosphorothioate and a 5′-$(CH_2)_6$-MMT-protected amino linker (Glen Research, Sterling, VA). This DNA was digested by T4 pol to remove the hydrolysis-sensitive R_p diastereomer (*1*). The amino-linked nonhydrolyzable DNA was incubated with rhodamine-X isothiocyanate (R-491, Molecular Probes, Eugene, OR) for 24 h at 37 °C with solution conditions as described (*2*). The labeled oligonucleotide was then separated from the unreacted free label using a P6 desalting column (Bio-Rad, Richmond, CA) and afterward from the unlabeled oligonucleotide using extended length polyacrylamide gels (*2*).

All primer−templates were annealed in buffer containing 25 mM Hepes (pH 7.5) and 50 mM NaCl. Reaction mixtures were heated to 90 °C and then slowly cooled to room temperature. When annealing was being carried out, template concentrations were adjusted to be 20% greater than primer concentrations. Some annealed primer−templates were further labeled with ^{32}P and analyzed by native polyacrylamide gel electrophoresis, revealing the absence of any free primer strands.

Methods

Steady-State Fluorescence Measurements. All steady-state fluorescence measurements were performed using a SPEX (Edison, NJ) 1681 Fluorolog spectrofluorimeter with excitation at 310 or 317.5 nm (±5 nm) for 2AP and 584 nm (±2 nm) for the rhodamine-X studies. Unless otherwise stated, all experiments were performed at 20 ± 2 °C.

Stopped-Flow Delivery and Fluorescence Detection System. The stopped-flow delivery system and detection are as described (*14*) except that data were collected from 1 to 20 ms per channel in 8000 total channels using either the FC-15 (31 μL) or the FC-08 (9 μL) cuvette (Molecular Kinetics, Pullman, WA). In experiments in which 2AP-containing DNA was used, the excitation wavelength was 317.5 nm and emission was collected through 360 nm cuton (L36, Hoya Optics, Fremont, CA) filters. For all experiments, delivery speeds were between 8 and 10 mL/s and multiple (10−25) runs were summed to increase the signal-to-noise ratio. In anisotropy binding experiments performed with rhodamine-X-labeled DNA, the FC-15 cuvette was used at a delivery speed of 8 mL/s. In experiments where 2AP-labeled DNA was used, the FC-08 cuvette was used at a delivery speed of 10 mL/s, with a measured dead time of 1.9 ± 0.4 ms. Experimental dead times were determined (not calculated) as described previously (*7*).

Stopped-flow anisotropy and total-intensity data were generated as follows:

$$r(t) = \frac{I_{||}G - I_{\perp}}{I_{||}G + 2I_{\perp}} \quad (1)$$

$$S(t) = I_{||}G + 2I_{\perp} \quad (2)$$

where $I_{||}$ and $I_{\perp}$ are the measured stopped-flow polarized fluorescence emission parallel and perpendicular to the excitation beam, respectively, and G is an instrumental polarization bias. The G factor was measured using horizontally polarized excitation and varied between 0.8 and 1.2 depending upon the experiment.

Protein and Mg^{2+} Concentration Dependence of the Hysteretic Transition. Reactions were initiated by mixing equal volumes (100 μL) of T4 pol solution with 2AP-containing ds primer−template DNA. Final reagent concentrations were 270 nM DNA, 0.1 mM EDTA, 25 mM Hepes, and 50 mM NaCl (pH 7.5). The final T4 pol protein concentrations were 70, 135, 270, and 540 nM. Single-stranded experiments were performed identically, except at only two T4 pol concentrations (70 and 270 nM). For Mg^{2+}-dependent studies, final Mg^{2+} concentrations were 0.1, 0.15, 0.4, and 8.0 mM, at a constant T4 pol concentration of 540 nM. Mg^{2+} was present in both protein and DNA solutions prior to mixing. Absolute final $MgCl_2$ concentrations were verified using a Molecular Probes Mg^{2+} calibration standard kit (product M-3120, Molecular Probes).

T4 Pol On-Rate and Off-Rate Experiments. Increasing concentrations of T4 pol were added (in the stopped flow) to a constant concentration of hydrolysis resistant rhodamine-X-labeled DNA. Final reaction conditions were 0.5 mM

DTT, 0.1 or 8 mM $MgCl_2$, 25 mM Hepes, and 50 mM NaCl (pH 7.5). T4 pol concentrations were 12.5, 25, 50, and 100 nM for 12.5 nM ss primers and 50, 100, and 200 nM for 25 nM ds primer−templates. On-rate and off-rate values (see below) were obtained by simultaneous analysis of all of the concentration-dependent on-rate data (together with the off-rate data) to determine internally consistent k_{on} and k_{off} values.

Off-rate experiments were performed by addition of a preincubated T4 pol−rhodamine-X-labeled hydrolysis resistant DNA complex to a heparin trap solution. The dissociation rate was determined from the decrease in the value of the steady-state anisotropy as the complex dissociated. Final reaction conditions were 12.5 nM DNA, 0.5 mM DTT, 0.1 mM $MgCl_2$, 25 mM Hepes, and 50 mM NaCl (pH 7.5). T4 pol and heparin concentrations used were 800 nM and 500 μg/mL for ds DNA experiments and 200 nM and 10 μg/mL for the ss DNA experiments. The observed dissociation kinetics were verified to be independent of heparin concentration. A nonlinear analysis of all of the data could be obtained using only a single bimolecular on rate and a unimolecular off rate. The methodology utilized for the numerical solutions of the binding equations can be found in previous works (*2*, *15*).

RESULTS

Identification of a Sigmoidal Time Course in the Excision of ds DNA. While equilibrium binding experiments are useful for quantitating multiple primer−template T4-bound states (*1*), they do not directly address the sequence of events involved in the processing of ss and ds DNA by T4 pol. To obtain this information, pre-steady-state kinetic studies were performed. The pre-steady-state kinetics of T4 pol excision of 2AP-containing DNA at optimal Mg^{2+} concentrations (8 mM) can be found in a companion study (*16*). In this study, emphasis is placed on precatalytic intramolecular events. These precatalytic events are essentially impossible to observe using pre-steady-state radioligand studies since they do not directly involve product formation, but mainly conformational transitions of the primer terminus within a bound T4 pol−DNA complex. It was found that, if T4 pol is added to ss or ds DNA at suboptimal Mg^{2+} concentrations ($\approx$0.1 mM), the excision rate is slow enough ($\approx$0.5 s^{-1}) that a clear separation of multiple precatalytic transitions can be observed.

The time course of the fluorescence enhancement of 2AP at the 3′-terminus of a primer in ds DNA clearly reveals three distinct phases upon interaction with T4 pol (Figure 1). Phase 1 consists of a 10 ms lag where no, or very slightly increasing, change in 2AP fluorescence intensity is evident. During phase 2 (centered at 22 ms), an increase in 2AP fluorescence intensity is observed which is sigmoidal in time. From previous work (*1*), it is known that this rising fluorescence intensity is associated with an elimination of base stacking of the 3′-end primer position within the exonuclease site of T4 pol, probably by the insertion of phenylalanine 120 (F120). The final phase of the reaction is a slow increase in intensity as 2AP is excised from the primer end, forming the 2-aminopurine monophosphate (inset of Figure 1). Only the slowest phase is accompanied by the characteristic drop in anisotropy associated with product formation (data not shown; see ref *7*).

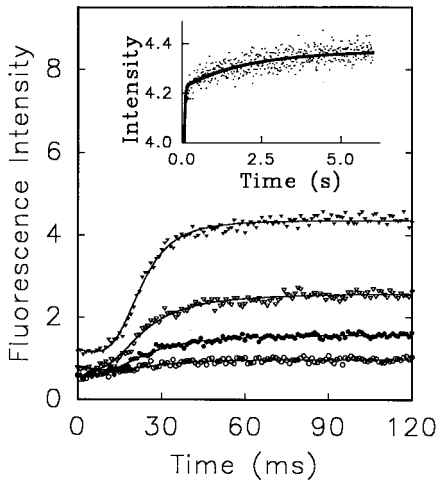

FIGURE 1: Identification of an intramolecular hysteretic kinetic step associated with the processing of ds DNA. Experiments were initiated by addition of T4 pol to 2AP-labeled ds DNA. The complete time course of the T4 pol−DNA interaction reaction is composed of an early 10 ms lag, a rapid 2AP fluorescence increase (centered at 22 ms), and a slow base excision reaction (upper inset). T4 pol concentrations were 67 (○), 134 (●), 268 (▽), and 536 nM (▼), with 266 nM ds DNA and 0.1 mM $MgCl_2$.

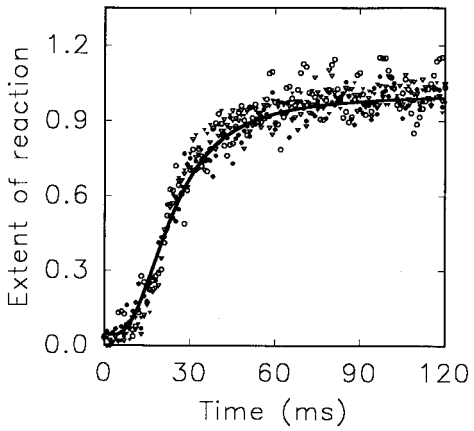

FIGURE 2: T4 pol concentration independence of the measured hysteretic profile. Plots of all T4 pol concentration experiments shown in Figure 2 were normalized to the extent of the reaction. T4 pol concentrations were 67 (○), 134 (●), 268 (▽), and 536 nM (▼), with 266 nM ds DNA and 0.1 mM $MgCl_2$.

To determine if the formation of the hyperfluorescent state (sigmoidal rise centered at 22 ms) was a second-order binding transition or an intramolecular conformational transition, the T4 pol concentration dependence was evaluated. Figure 2 reveals that, when the T4 pol concentration is varied 8-fold, no change in the lag phase or the rate of the intensity increase was observed. Nonlinear analysis of each individual sigmoidal transition yielded a half-maximal response time of 22 $\pm$ 1 ms. These experiments indicate that the sigmoidal transition is intramolecular, involving conformational changes induced in the primer end after T4 pol is bound to the DNA. Further experiments (anisotropy data described below) will directly examine the coupling between protein binding and this intramolecular base-unstacking reaction. An identical lag and sigmoidal shape were also observed for T4 pol addition to a terminally mismatched (2AP base-paired with cytosine) p/t end (data not shown).

Identical experiments performed on ss 2AP primers failed to reveal any of the kinetic complexity observed with the

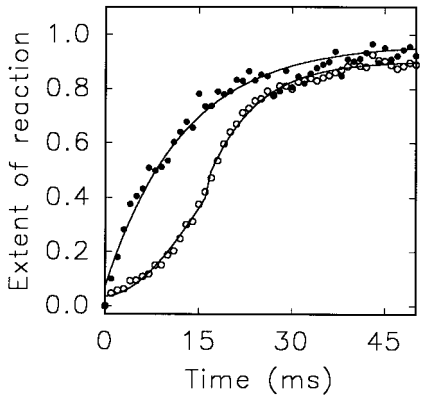

FIGURE 3: Direct comparison of the intramolecular 2AP fluorescence enhancement observed with single-stranded (●) and double-stranded (○) DNA. The fit shown with the ds DNA transition was generated using eq 3 for a hysteretic lag combined with a first-order transition as described in the Discussion. Conditions for these experiments were 266 nM DNA (ds or ss primer), 100 μM $MgCl_2$, 25 mM Hepes, 50 mM NaCl (pH 7.5), and 536 nM T4 pol.

p/t DNA. The data in Figure 3 represent stopped-flow experiments for ss and ds DNA collected "back to back" within minutes of each other, to ensure that all operational parameters of the stopped flow were as closely matched as possible (e.g., instrumental dead times, flow rates, enzyme aging, etc.). The ss DNA transition clearly lacks both the kinetic lag and sigmoidal-shaped intensity increase found in p/t DNA, and can be adequately described using a single-exponential function (Figure 3).

Kinetics of Assembly of T4 Pol onto ss and ds DNA. To perform a rigorous comparison of the ss and ds DNA exonuclease experiments (as in Figure 3), it is important to know the absolute assembly rates (on rates) of T4 pol to ss primers and ds primer−templates. The kinetic lag and sigmoidal transition which appear to be missing in ss DNA could be the result of faster binding "pushing" the lag phase into the dead time of the stopped flow, with only the slower exponential increasing phase of the hysteretic transition being observable. To directly measure the on rates for both ss and ds DNA, stopped-flow fluorescence anisotropy binding experiments were performed (see Methods). In this manner, the coupling between protein binding and the internal DNA base-unstacking transition can be directly measured.

Equilibrium binding, on-rate, and off-rate rhodamine-X anisotropy experiments were performed on both ss and ds p/t DNA. Nearly identical kinetic and equilibrium binding properties were observed for both ds DNA (Figure 4A,B) and ss primers (data not shown). Upon binding by T4 pol, the steady-state anisotropy value for rhodamine-X-labeled ds DNA increases from 0.16 to 0.32 (Figure 4A) and that of ss DNA from 0.10 to 0.28. A single dissociation constant of 21 nM is recovered from the equilibrium binding analysis of the ss (data not shown) or ds DNA data (Figure 4A). Association rates were measured over a 4-fold change in T4 pol concentration (at both 0.1 and 8 mM Mg^{2+}). These data sets were simultaneously analyzed (at each Mg^{2+} concentration) in terms of internally consistent on rate(s). These data could be adequately described using a single bimolecular on rate (smooth lines in Figure 4B for 8 mM Mg^{2+}). At 100 μM Mg^{2+}, essentially identical on rates were obtained for both ss (4.5×10^8 M^{-1} s^{-1}) and ds DNA (4.7×10^8 M^{-1} s^{-1}). These results clearly prove that the differences

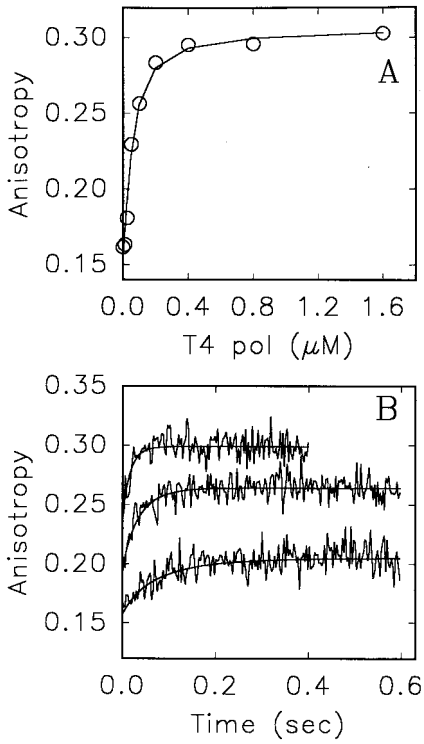

FIGURE 4: Equilibrium (A) and kinetic (B) determination of the properties of binding for T4 pol binding to ds DNA. These experiments were performed using rhodamine-X-labeled ds DNA and fluorescence anisotropy detection as in Methods. (A) Equilibrium isotherm for binding of T4 pol to ds DNA. The solid line is a nonlinear fit using a single dissociation constant of 21 nM. Conditions were 8 mM $MgCl_2$, 0.1 mM EDTA, and 50 nM nonhydrolyzable (*1*) ds DNA. (B) Stopped-flow kinetics of the binding of T4 polymerase to rhodamine-X-labeled ds DNA. Fits shown are from a global simultaneous nonlinear analysis (as discussed in Methods) using a single second-order rate constant of 1.0×10^8 M^{-1} s^{-1}. Conditions were 8 mM $MgCl_2$, 0.1 mM EDTA, 25 nM ds DNA, and 50, 100, and 200 nM T4 pol.

in shapes associated with the formation of the hyperfluorescent state (Figure 3) are not due to differences in intrinsic second-order binding rates. The on-rate value for ds DNA obtained at 8 mM Mg^{2+} was lower (1×10^8 M^{-1} s^{-1}).

For off-rate determination, preincubated T4 polymerase and rhodamine-X-labeled DNA were mixed with either a heparin trap or excess nonlabeled p/t DNA. An identical exponential decrease in anisotropy was observed for either method of T4 pol dissociation (data not shown). Identical off rates of T4 pol were obtained for both ss and ds DNA (k_{off} = 9.3 s^{-1}, with 100 μM Mg^{2+}). The ratio of the measured on rate and off rate yields a (kinetically determined) dissociation constant for the T4 pol complex of 20.7 nM; a value of 21 nM was obtained from the fit to the equilibrium binding data (Figure 4A). The internal consistency of the kinetic and equilibrium binding results indicates that the measured on and off rates are an adequate description of the T4 pol−DNA interaction process.

The independently measured on and off rates can be used to calculate the time dependence of the fraction of DNA bound for both the ss and ds 2AP base-unstacking experiments. Comparison of the calculated fraction of bound ds DNA as a function of time (Figure 5A, dashed lines) to the sigmoidal excision time reveals that the majority of binding occurs during the lag phase which precedes the primer terminus base-unstacking event. Thus, the sigmoidal transi-

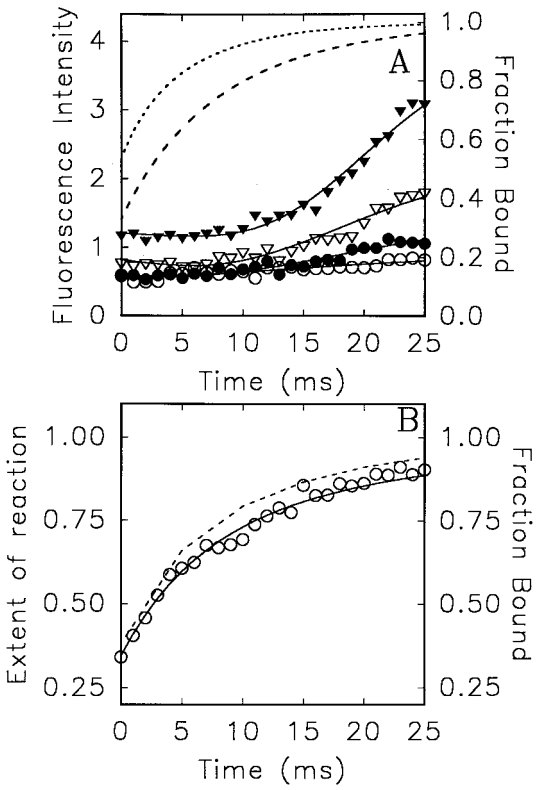

FIGURE 5: Comparison of kinetics of second-order binding of T4 pol to ds (A) and ss (B) DNA with respect to the intramolecular 2AP fluorescence enhancement kinetics at 100 μM Mg^{2+}. The fraction bound was calculated using on- and off-rate values obtained from the rhodamine-X stopped-flow anisotropy experiments (Figure 4). (A) 2AP fluorescence enhancement as a function of T4 pol concentrations: 67 (○), 134 (●), 268 (▽), and 536 nM (▼). The fraction of T4 bound is calculated from the measured on rate of 4.6×10^8 M^{-1} s^{-1} at 67 (− −) and 536 nM (--) T4 pol. (B) 2AP fluorescence enhancement observed with ss DNA. The dashed line represents the fraction of the T4 pol−ss DNA complex formed using the measured on rate. Conditions were 266 nM ss primer, 0.1 mM $MgCl_2$, 25 mM Hepes, 50 mM NaCl (pH 7.5), and 268 nM T4 pol.

tion is an intramolecular reaction and independent of the T4 pol concentration as previously observed in Figure 2. This binding result explains why the ds DNA sigmoidal transition was concentration-independent (Figure 2). The ss 2AP time course (Figure 5B), however, reveals that binding and the 2AP fluorescence enhancement transition are nearly coincident.

Investigation of the Mg^{2+} Dependence of the Hysteretic 2AP Fluorescence Enhancement. The Mg^{2+} dependence of the hysteretic lag and formation of the hyperfluorescent state in ds DNA was examined. Figure 6 shows that, as the Mg^{2+} concentration increases, the initial portion of the sigmoidal time course becomes substantially more rapid and by 8 mM $MgCl_2$ has disappeared completely, moving within the 1.9 ms dead time of the stopped-flow apparatus. Nonlinear analysis of the measured hysteretic transitions resolves composite rate constants for hysteresis (k_1 of eq 3, see below) of 55, 72, and 110 s^{-1} at 100, 150, and 400 μM $MgCl_2$, respectively. A single Mg^{2+}-independent first-order rate constant of 130 s^{-1} (k_2 of eq 3) described all of the data sets after completion of the hysteretic lag. Data obtained at 8 mM Mg^{2+} no longer had a visible lag or sigmoidal appearance and could be adequately described using a single first-order rate constant of approximately 130 s^{-1}.

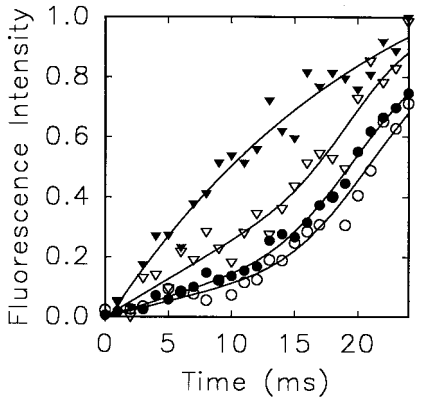

FIGURE 6: Evaluation of the Mg^{2+} dependence of the lag phase in the 2AP fluorescence enhancement which is observed preceding catalysis. Experiments were initiated by addition of T4 pol to 2AP-labeled hydrolyzable ds DNA. Mg^{2+} concentrations were 100 μM (○), 150 μM (●), 400 μM (▽), and 8 mM (▼) $MgCl_2$. Conditions were 266 nM ds DNA, 25 mM Hepes, 50 mM NaCl (pH 7.5), and 536 nM T4 pol.

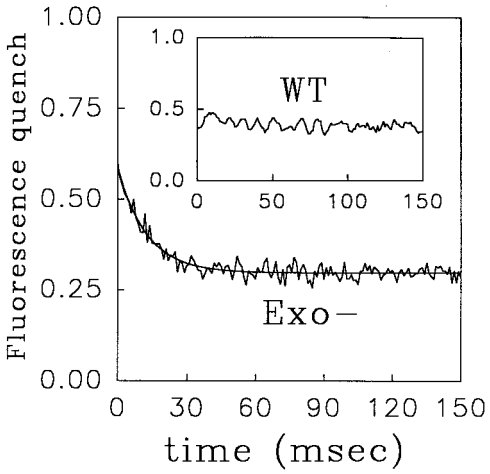

FIGURE 7: Kinetics of the Mg^{2+}-induced transition from the base-unstacked 2AP primer terminus in the exonuclease site to a base-stacked configuration partitioned in both the exonuclease and polymerase sites. Exonuclease-deficient D112A/E114A (Exo−) T4 pol (0.6 μM) is prebound to hydrolysis resistant p/t (200 nM, 17mer−30mer; see ref *1*; 1 mM NaCl, 0.5 mM EDTA, and 0.5 mM DTT) to generate the hyperfluorescent state (all kinetic signals normalized to this "preshot" value). Reaction is initiated by addition of 16 mM Mg^{2+}. The rate determined for this transition is 80 s^{-1}. (Inset) Identical reactions carried out with WT T4 pol occur within the dead time of the stopped flow (≈2 ms).

Kinetics of the Mg^{2+}-Induced 2AP Fluorescence Quench: The Base-Unstacked to Base-Stacked Transition. In Beechem et al. (*1*), it was shown that, at high Mg^{2+} concentrations, the unstacked primer terminus is pushed out of the exonuclease active site and becomes redistributed between an exonuclease "dark" state and a polymerase highly quenched state. Stopped-flow experiments were performed at high Mg^{2+} concentrations to examine the kinetics of this "base-restacking" reaction. Experiments performed with WT T4 revealed that, at 8 mM Mg^{2+}, the base-restacking reaction occurs within the dead time of the stopped flow (k > 200 s^{-1}, Figure 7 inset). In a companion study (*16*), this high-Mg^{2+} concentration quenching phase is kinetically resolved. Experiments performed on the exonuclease-deficient T4 pol mutant (D112A/E114A), however, allowed the resolution of the kinetics of the base-restacking transition (Figure 7). A monophasic decrease in 2AP fluorescence was observed

which could be fit to a single-exponential transition of 80 s^{-1} (smooth line in Figure 7). Identical experiments performed with a terminally mismatched primer end (2AP−cytosine) yielded the same monophasic transition ($k = 85$ s^{-1}, data not shown).

DISCUSSION

The pre-steady-state kinetics and time lags associated with the processing of the 3′-primer position of ds DNA (shown in Figures 1−3, 5, and 6) are clearly sigmoidal in character. Sigmoidal kinetics of this type were originally termed enzyme hysteresis (*17*), using as a definition for hysteresis "the time lag exhibited by a body in reacting to outside forces." Sigmoidal kinetics of this type can occur whenever an enzyme exists in two or more conformational forms which differ in some catalytic or binding sense (*17*). Hence, simple examination of the shape of the observed kinetics in this study provides unequivocal support for the equilibrium interpretation of multiple highly populated conformational states associated with the primer terminus. Under suboptimal conditions (in this case low Mg^{2+} concentrations), the interconversion between these two conformational forms becomes rate-limiting, resulting in the characteristic hysteretic lag (*17*).

Two sets of measurements revealed that the two conformational forms of the enzyme (minimum required to produce hysteresis) were associated with DNA-bound states, and not associated with multiple conformations of the unligated protein. The measured initial binding event (Figure 4A,B) was adequately described by single on and off rates, implying that the conformational heterogeneity which is observed originates after binding. Similarly, the protein concentration independence of the hysteretic transition (Figure 2) supports the argument that the two conformational forms of T4 pol are bound to DNA.

In the original description of enzymatic hysteresis, Frieden (*17*) notes that, if a hysteretic step is followed by a first-order rate process, an overall sigmoidal-shaped reaction time course is expected. Therefore, it should be possible to describe the reaction time courses (Figures 2−4, 6A, and 7) using the following equation (adapted from eqs 10 and 11 of ref *17*):

$$F_{obs}(t) = v_f\left[t - \frac{1}{k_1}[1 - \exp(-k_1 t)]\right] + \alpha[1 - \exp[-k_2(t - t_2)]] \quad (3)$$

where $F_{obs}(t)$ is the fluorescence observed at time t, k_1 is the composite rate (for the hysteretic step) which depends on Mg^{2+} concentration, v_f is reaction velocity at the end of the hysteretic lag phase, α is the amplitude of the first-order process and is forced to zero when $t < t_2$, t_2 is the time when the hysteretic lag is complete, and k_2 is the rate constant of the first-order process occurring after the hysteretic lag. The first term describes the hysteretic lag, and the second describes the first-order process which follows the lag. This function can be used to adequately describe the sigmoidal reaction time course (e.g., smooth line fit in Figures 1−3, 5A, and 6). A single value of 130 s^{-1} for k_2 was found to adequately describe all of the kinetic data (independent of protein or Mg^{2+} concentration). The hysteretic transition composite rate, however, was Mg^{2+}-dependent, yielding values of 55, 72, and 110 s^{-1} for k_1 at 100, 150, and 400 μM $MgCl_2$, respectively (Figure 6 fits). It should be emphasized that the hysteretic fitting parameter, k_1, is essentially empirical in nature, and no attempt has been made to generate a detailed kinetic model, which from first principles generates the observed Mg^{2+} dependence.

Less empirical fitting of the data was attempted, using nonlinear least-squares optimization of a numerical solution to the differential equations associated with second-order binding, followed by a sequence of first-order transitions. When one constrains the fitting of such a model to obey spectroscopic rules (e.g., no states can generate "negative photons"), a very large number of intermediates ($\approx$5) are required before a truly sigmoidal shape is generated. Nonlinearly optimized fitting using only one or two intermediate states resulted in dramatically inferior fits with fitting variances that were >5 times larger than the empirical sigmoidal model. The requirement for many rather "ill-defined" intermediate states led us to abandon this type of modeling at the current time.

Crucial for the rigorous interpretation of the kinetic differences associated with the processing of ss primers and ds primer−templates are high accuracy binding measurements. Stopped-flow anisotropy experiments performed on rhodamine-X-labeled DNA revealed the precise time course for assembly of T4 pol onto both ss and ds DNA. Overlapping the measured time courses for T4 pol assembly (rhodamine-X anisotropy signal) and primer end base unstacking (2AP fluorescence increase signal) clearly reveals the essential differences associated with the processing of ss primers and the processing of ds primer−templates (Figure 5). Single-stranded primer base-unstacking reactions are clearly not rate-limiting, as revealed by the near superposition of the DNA binding and base-unstacking signal changes (Figure 5B). The processing of ds primer−templates, however, is a much more complex reaction, and becomes rate-limited by an intramolecular Mg^{2+}-dependent step which occurs after T4 pol is bound (Figure 5A). This additional intramolecular conformational transition is not a single first-order process, which would still yield exponential type kinetics. To observe a hysteretic lag of this type, a severely rate-limiting multistep transition is required.

The primer base "restacking" reaction which occurs at high Mg^{2+} concentrations (>100 μM) was also examined. This quenching transition was proposed in the previous study (*1*) to involve the loss of phenylalanine 120 base intercalation upon Mg^{2+} binding (see Figure 8 of ref *1*). With WT T4 pol, this transition is very rapid (resolved in ref *16*). Examination of the exo$^-$ (D112A/E114A) T4 mutant, however, allowed characterization of this transition, which was found to be monophasic ($k = 80$ s^{-1}) and independent of the base pairing of the primer terminus.

Crucial for the interpretation of this complex kinetic transition is an understanding of the types of protein−DNA states which link these various kinetic species. From the time-resolved fluorescence study in the preceding paper (*1*), the highly fluorescent state was found to be associated with an unstacked primer terminal 2AP located in the exonuclease active site. This unstacked primer terminus probably originates from the insertion of phenylalanine 120 into the primer strand just 5′ of the primer terminus in a manner exactly

analogous to that observed in the crystal structure of the RB69 DNA polymerase (*18*). Therefore, the T4 pol−primer−template state at the end of the hysteretic transition is reasonably well defined. A key question is therefore the following. In which binding site is the primer terminus located during the initial phase of the reaction (i.e., the first 10 ms)? Since these primer−templates are so small (17mer−30mer), the "scanning time" for searching along the DNA for the primer end should be essentially instantaneous. Examination of the lag time for a slightly larger p/t DNA (27mer−40mer, 60% larger ds region) yielded identical lag times and hysteretic profiles (data not shown), consistent with this assumption. Hence, the lag time is probably not associated with a DNA polymerase "scanning" rate.

Therefore, the binding site of the initially bound p/t terminus must be located within either the polymerase or exonuclease active site. The only other alternative is that, before the p/t end is associated with either the polymerase or exonuclease binding sites, a (as yet uncharacterized) binding site exists which then "channels" the p/t end to either location. In the absence of any data characterizing such an intermediate DNA binding site, we will assume the p/t end is located in either the polymerase or exonuclease binding site, or some fractional component in each.

The primer−template end of the 2AP-T ds DNA would be expected to partition significantly more into the exonuclease site of T4 pol than a correct A-T base pair. The 2AP-T end may be destabilized in the exonuclease active site by more than 1 kcal/mol compared to a correct A-T base pair (*19*, *20*). The origin of the 2AP-T destabilization has been hypothesized to reside in the exclusion of water from the enzyme-bound state (*21*). Hence, these studies with AP-T base pairs represent a "slightly biased" (toward-the-exonuclease site) view of the polymerase−exonuclease partitioning compared to correct A-T base pairs.

Direct comparison of ss DNA and ds DNA binding kinetics clearly resolves a fundamental difference between the processing of primer ends for these two forms of DNA (Figures 3 and 5). If the 2AP-T ds DNA primer terminus entered the exonuclease site in exactly the same manner as ss 2AP-DNA, then the ds data (Figure 5A) would have a large fractional component identical to the ss DNA transition (Figure 5B). Clearly, this result is not observed, as the ds DNA signal shows a definite lag with no fraction of a hyperbolic increase in fluorescence intensity linked to the binding kinetics.

In the simplest of models, one could hypothesize that the initial binding state of the ds primer−template is at the polymerase site. This site is known to have a very quenched 2AP fluorescence (*1*) and would hence show no fluorescence enhancement upon T4 pol binding. The rate of the measured 2AP fluorescence enhancement, therefore, would directly correspond to the polymerase to exonuclease switching rate. Extrapolation of the measured hysteretic composite rate (k_1) at 100, 150, and 400 mM Mg^{2+} to maximal enzyme activity concentrations of Mg^{2+} yields a predicted value of nearly 1400 s^{-1} with 8 mM Mg^{2+}. This extrapolation assumes k_1 would increase linearly from 0.4 to 8 mM Mg^{2+}, and hence represents an upper limit for the rate of this process. Therefore, the range of rate constants associated with the 2AP fluorescence enhancement in ds p/t DNA is as follows: 110 s^{-1} (400 mM Mg^{2+} measured) < k_1 < 1400 s^{-1} (8 mM Mg^{2+} linear extrapolated rate). This rate constant (either measured or extrapolated) is several orders of magnitude larger than the 1−5 s^{-1} rates previously proposed for polymerase to exonuclease switching frequencies (*22*−*24*).

If the polymerase to exonuclease switching frequencies were as low as 1−5 s^{-1}, however, this switching process would be rate-limiting, when compared to the known maximal polymerization (400 s^{-1}) and excision rates (100 s^{-1}) in T4 pol (*23*). Two kinetic partitioning studies have shown that between 8 and 25% of the total correct nucleotides incorporated are hydrolyzed by the T4 polymerase (*9*, *20*). This number is approximately the ratio of maximal excision and polymerization rates (100 s^{-1}/400 s^{-1}). A simple interpretation of the similarity between the kinetic partitioning results and the ratio of the polymerization and exonuclease rate constants would indicate that the switching rate between the polymerase and exonuclease sites is not rate-limiting for T4 pol in vivo. The rapid hysteretic rates (k_1) measured in this study, when interpreted as a direct measure of polymerase to exonuclease switching, are consistent with the original kinetic partitioning data of Clayton et al. (*20*) and Reha-Krantz and Nonay (*9*). Given the large percentage of nucleoside triphosphates turned over by T4 polymerase, this number is also more consistent with the known rapid rates of replication in vivo.

If the previously measured slower switching rates (1−5 s^{-1}) are correct (*22*−*24*), then the measured fast hysteretic transition found in ds DNA must not be associated with a polymerase to exonuclease switching rate, but rather with conversion of a base-stacked primer terminus to an unstacked primer terminus directly within the exonuclease binding site. This interpretation requires the presence of an exonuclease bound dark state, where the 2AP primer terminus is significantly base-stacked, yet still within the exonuclease binding site. Evidence for such a dark state (Exo_D) was found in the equilibrium time-resolved fluorescence study (*1*), so this type of result is possible. The time lag associated with the hysteretic transition would therefore represent the time scale required to position the 3′-primer end into the "first-staging" area of the exonuclease site. This staging area would be involved in positioning the 3′-primer end into a configuration which allows the base-unstacking, phenylalanine intercalation, transition to occur. To produce the type of hysteretic transition which is observed, this positioning reaction must be a complex multistep process, which is severely compromised in the presence of low Mg^{2+} concentrations. Once the 3′-primer end is in a proper configuration to base-unstack, the actual base-unstacking transition occurs with a Mg^{2+}-independent rate of ≈130 s^{-1} (Figure 3, first-order transition region).

It is interesting to note that sigmoidal 2AP fluorescence enhancement kinetics, with nearly exactly the same shape as that observed in this study, have been previously observed for the kinetics of open complex formation by bacteriophage T7 RNA polymerase (see ref *25*, Figure 3). The overall time scale for 2AP fluorescence enhancement in T7 RNA polymerase, however, is in the kilosecond time regime, as opposed to the millisecond regime found in this study of T4 DNA polymerase. Nonetheless, the near identity of the 2AP kinetic response shapes suggests that the rate-determining step occurring in T4 pol at low Mg^{2+} concentrations may

be similar to that occurring in the strand separation reactions of RNA polymerases. The striking kinetic similarity suggests that a common rate-limiting step may be operational in both enzymes as they separate paired DNA strands.

The presence of the hysteretic shape ensures that at least two conformationally distinct T4 pol-bound states are populated when processing ds primer−templates (consistent with the equilibrium study of ref *1*). Whether this hysteretic reaction represents a polymerase to exonuclease switching transition, or simply a multistep base-unstacking reaction in the exonuclease active site, will only be determined by further experimentation on this system.

ACKNOWLEDGMENT

M.R.O. and J.M.B. acknowledge helpful discussions concerning hysteretic behavior in enzymes with Dr. Paul Bock (Vanderbilt University). Prof. Linda Reha-Krantz (University of Alberta, Edmonton, AB) is acknowledged for the generous supply of WT and mutant enzymes and for critical reading of the manuscript.

REFERENCES

1. Beechem, J. M., Otto, M. R., Bloom, L. B., Eritja, R., Reha-Krantz, L. J., and Goodman, M. F. (1998) *Biochemistry 37*, 10144−10155.
2. Perez-Howard, G. M., Weil, P. A., and Beechem, J. M. (1995) *Biochemistry 34*, 8005−8017.
3. Dunkak, K. S., Otto, M. R., and Beechem, J. M. (1996) *Anal. Biochem. 243*, 234−244.
4. Bloom, L. B., Turner, J., Kelman, Z., Beechem, J. M., O'Donnell, M., and Goodman, M. F. (1996) *J. Biol. Chem. 293*, 30699−30708.
5. Ward, D. C., Reich, E., and Stryer, L. (1969) *J. Biol. Chem. 244*, 1228−1237.
6. Bloom, L. B., Otto, M. R., Beechem, J. M., and Goodman, M. F. (1993) *Biochemistry 32*, 11247−11258.
7. Bloom, L. B., Otto, M. R., Eritja, R., Reha-Krantz, L. J., Goodman, M. F., and Beechem, J. M. (1994) *Biochemistry 33*, 7576−7586.
8. Spicer, E. K., Rush, J., Fung, C., Reha-Krantz, L. J., Karam, J. D., and Konigsberg, W. H. (1988) *J. Biol. Chem. 263*, 7478−7486.
9. Reha-Krantz, L. J., and Nonay, R. L. (1994) *J. Biol. Chem. 269*, 5635−5643.
10. Nossal, N. G. (1994) in *Molecular Biology of Bacteriophage T4* (Karam, J. D., Drake, J. W., et al., Eds.) pp 43−54, American Society for Microbiology, Washington, DC.
11. Reha-Krantz, L. J., and Nonay, R. L. (1993) *J. Biol. Chem. 268*, 27100−27108.
12. Reha-Krantz, L. J., Stocki, S., Nonay, R. L., Eliosa, Dimayuga, E., Goodrich, L. D., Konigsberg, W. H., and Spicer, E. K. (1991) *Proc. Natl. Acad. Sci. U.S.A. 88*, 2417−2421.
13. Connolly, B. A. (1991) in *Oligonucleotides and analogs: A practical approach* (Eckstein, F., Ed.) pp 162−168, IRL Press, Oxford, England.
14. Otto, M. R., Lillo, M. P., and Beechem, J. M. (1994) *Biophys. J. 67*, 2511−2521.
15. Rousseau, D. L., Jr., Staros, J. V., and Beechem, J. M. (1995) *Biochemistry 34*, 14508−14518.
16. Reha-Krantz, L. J., Marques, L. A., Elisseeva, E., Baker, R. P., Bloom, L. B., Dunford, B., and Goodman, M. F. (1998) *J. Biol. Chem.* (in preparation).
17. Frieden, C. (1970) *J. Biol. Chem. 245*, 5788−5799.
18. Wang, J., Sattar, A. K. M. A., Wang, C. C., Karam, J. D., Konigsberg, W. H., and Steitz, T. A. (1997) *Cell 89*, 1087−1099.
19. Galas, D., and Branscomb, E. (1978) *J. Mol. Biol. 124*, 653−687.
20. Clayton, L. K., Goodman, M. F., Branscomb, E. W., and Galas, D. J. (1979) *J. Biol. Chem. 254*, 1902−1912.
21. Petruska, J., Sowers, L. C., and Goodman, M. F. (1986) *Proc. Natl. Acad. Sci. U.S.A. 83*, 1559−1562.
22. Donlin, M. J., Patel, S. S., and Johnson, K. A. (1991) *Biochemistry 30*, 538−546.
23. Capson, T. L., Peliska, J. A., Kaboord, B. F., Frey, M. W., Lively, C., Dahlberg, M., and Benkovic, S. J. (1992) *Biochemistry 31*, 10984−10994.
24. Marquez, L. A., and Reha-Krantz, L. J. (1996) *J. Biol. Chem. 271*, 28903−28911.
25. Sastry, S. S., and Ross, B. M. (1996) *Biochemistry 35*, 15715−15725.

BI9800754